THE JOURNAL OF PHYSICAL CHEMISTRY LETTERS
A JOURNAL OF THE AMERICAN CHEMICAL SOCIETY

pubs.acs.org/JPCL

Letter

Precision Measurement of the Electron Affinity of Chlorine via High-Resolution Photoelectron Spectroscopy

Shuaiting Yan, Rui Zhang, and Chuangang Ning*

Cite This: J. Phys. Chem. Lett. 2024, 15, 7735−7739

Read Online

ACCESS | Metrics & More | Article Recommendations | Supporting Information

ABSTRACT: Chlorine (Cl_2) is a diatomic molecule used as an important industrial gas. However, the electron affinity (EA) of Cl_2, a fundamental parameter for understanding chemical reactions, has no accurate experimental result available. The latest result of the EA value of Cl_2 is 2.50(20) eV reported in 1983. In the present work, we report the precision measurement of the EA of Cl_2 with the successive difference method via the high-resolution photoelectron spectroscopy of cryogenically cold chlorine anions Cl_2^-. The EA of Cl_2 is determined to be 19432(9) cm^{-1} or 2.4093(11) eV.

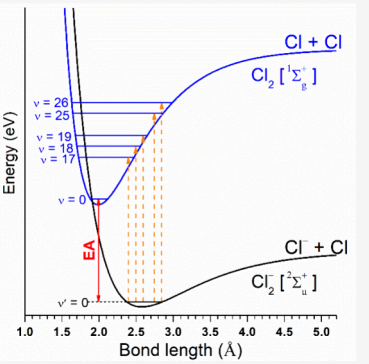

Halogen elements exist stably in nature as homonuclear diatomic molecules (F_2, Cl_2, Br_2, I_2). The electron affinity (EA) is a fundamental parameter of an atom or molecule, measuring its capability to form the corresponding negative ion.[1,2] Like the ionization potential (IP), EA is an important parameter for understanding chemical reactions. Most EA values of the common molecules and atoms have been accurately measured via the photoelectron spectroscopy.[1−4] For example, EA(O_2)=0.448(6) eV,[5] and EA(I_2) =2.524(5) eV.[6] Chlorine is a common gas. High accurate EA value of Cl_2 is crucial for understanding many chemical and physical processes.[7−9] Surprisingly, no accurate experimental EA value of Cl_2 is available. The possible reason is the significant bond-length change when photodetaching Cl_2^-, which results in unfavorable Franck−Condon factors and quasi-continuous spectra, thus it is difficult to make a definitive assignment.[10−12]

In past decades, the EA value of Cl_2 has indirectly been estimated through experiments or calculated theoretically.[13−17] Lacmann et al. reported the EA value of Cl_2 as 3.20(20) eV in 1970 through experimental investigations involving the collisional excitation and ionization of potassium atom interacting with several diatomic molecules, such as HCl, Cl_2, Br_2, CO, NO, and O_2.[18] Subsequently, the EA value of Cl_2 was revised to 2.38(10) eV by measuring the energy thresholds for the charge-transfer process of two endoergic reactions $I^- + Cl_2 \rightarrow Cl_2^- + I$ and $Br^- + Cl_2 \rightarrow Cl_2^- + Br$.[19] Concurrently, Tiernan's group utilized a tandem mass spectrometer to measure translational energy thresholds of electron transfer reactions from various atomic negative ions to Cl_2 and integrated this data with known thermodynamic data to determine the EA value of Cl_2 as 2.32(10) eV.[20] However, Hubers and co-workers investigated alkali metal atoms (Na, K, Cs) colliding with halogen molecules to form negative ions, determining the EA value of Cl_2 to be 1.02 ± 0.05 eV based on the positions of Landau−Zener maxima in total cross sections for negative ion formation.[21] Later, Bowen et al. conducted a similar experimental approach, employing two supersonic beams: one to produce fast alkali atoms and another to produce the Cl_2 molecular cluster. They derived the EA value of Cl_2 as 2.50(20) eV from the threshold energy for ion-pair formation.[17]

The present work aims to precisely determine the EA value of Cl_2 using the cryogenically slow-electron velocity-map imaging (cryo-SEVI) method. Details of our cryo-SEVI apparatus can be found elsewhere.[22−27] In this study, Cl_2^- anions were produced by expanding trace amounts of CCl_4 with methane gas (∼1 MPa) through a pulsed valve equipped with a filament ionizer.[28] The nascent Cl_2^- anions were directed through a hexapole ion guide, then collected and cooled in a radio frequency (RF) ion trap mounted on the second stage of closed-cycle helium refrigerator, with a nominal temperature of 8 K. The trapped anions were cooled down to their ground vibrational states after sufficient collisions with a buffer gas (20% H_2 and 80% He) for 45 ms, and were subsequently released into the extraction region

Received: June 19, 2024
Revised: July 16, 2024
Accepted: July 18, 2024
Published: July 24, 2024

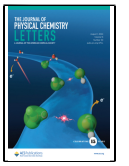

https://doi.org/10.1021/acs.jpclett.4c01821
J. Phys. Chem. Lett. 2024, 15, 7735−7739

of a Wiley−McLaren type time-of-flight (TOF) mass spectrometer.[29] The Cl_2^- anions with mass m = 70 were selected and intercepted by a detachment laser in the interaction region of velocity map imaging (VMI).[30] Photodetachment was performed using a tunable laser from the signal light of an optical parametric oscillator (OPO, 210−405 nm, line width ∼6 cm^{-1}) pumped via a Quanta-Ray Lab 190 Nd: YAG laser operating at 20 Hz. The photodetached electrons were projected onto a set of microchannel plates coupled with a phosphor screen and recorded using a charge-coupled device (CCD) camera. Energy calibration was carried out using the known spectra of $^{35}Cl^-$ at various photon energies.[31] The projected 2D photoelectron image was used to reconstructed the 3D photoelectron distribution via the maximum entropy velocity Legendre reconstruction (MEVELER) method.[32] The cryo-SEVI exhibits very high energy resolution for low-kinetic-energy photoelectrons, typically a few cm^{-1} near the photodetachment threshold.[33]

Figure 1 displays the photoelectron energy spectrum of Cl_2^- anions, recorded at the wavelength of 300 nm. The spectrum

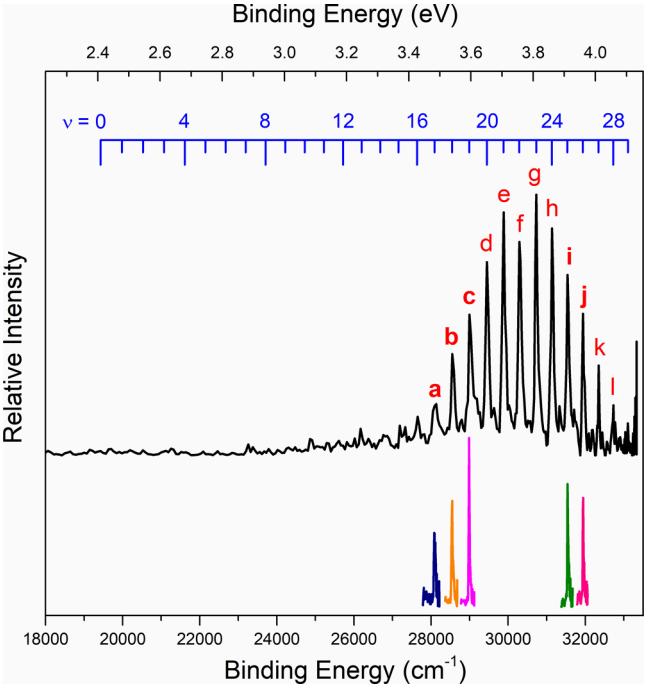

Figure 1. Overview cryo-SEVI spectra of Cl_2^- (black) and the high-resolution peaks obtained near the respective photodetachment thresholds (under the curve, in color). The vertical bars above the curve indicate the vibrational quantum number.

contains a series of peaks labeled as *a-l*, representing the transitions from the anionic ground state $X'\ ^2\Sigma_u^+$ to a series of vibrationally excited states of the neutral ground state $X\ ^1\Sigma_g^+$. Due to the extremely low Franck−Condon factor between the neutral vibrational ground state and the anionic vibrational ground state, the band origin (0 ← 0 transition) cannot be observed. Otherwise, the EA value of Cl_2 can be directly measured via the 0 ← 0 transition. Given the well-established vibrational energy levels of Cl_2, definitive assignment of a peak to a specific vibrational quantum number v would allow for the determination of EA(Cl_2) from the corresponding vibrationally excited state. The energy level of a diatomic rotor is conveniently written in the Dunham form:[34]

$$F_{\nu K} = \sum_{lj} Y_{lj}\left(\nu + \frac{1}{2}\right)^l K^j(K+1)^j \quad (1)$$

where ν and K are the vibrational and rotational quantum numbers, respectively. The first subscript l under the coefficients Y_{lj} refers to the power of the vibrational quantum number, the second j to that of the rotational quantum number. Since we cannot resolve rotational states and we expect that the rotational profile has no significant impact on the energy interval since the rotational profile for each vibrational peak in Figure 1 is almost the same, the rotational quantum number j was set to 0 for simplicity. Therefore, the vibrational energy level of Cl_2 is given by

$$E_\nu = Y_{10}\left(\nu + \frac{1}{2}\right) + Y_{20}\left(\nu + \frac{1}{2}\right)^2 + Y_{30}\left(\nu + \frac{1}{2}\right)^3 + Y_{40}\left(\nu + \frac{1}{2}\right)^4 + Y_{50}\left(\nu + \frac{1}{2}\right)^5 + Y_{60}\left(\nu + \frac{1}{2}\right)^6 + Y_{00} \quad (2)$$

The coefficients Y_{lj} of the neutral Cl_2 ($X\ ^1\Sigma_g^+$) have been determined via the resonance fluorescence spectrum,[35] as listed in Table S1 of the Supporting Information. The typical uncertainty of the vibrational energy level is less than 0.1 cm^{-1}. The connection between the coefficients Y_{lj} and the spectroscopic constants is $Y_{10} \sim \omega_e$, $Y_{20} \sim -\omega_e\chi_e$, $Y_{30} \sim -\omega_e y$, and $Y_{40} \sim \omega_e z$.

Due to the small value of the anharmonic constant $\omega_e\chi_e$ (2.67 cm^{-1}) for neutral Cl_2 ($X\ ^1\Sigma_g^+$), it becomes challenging to assign peaks *a-l* solely by comparing the energy intervals between two adjacent peaks with those given by eq 2. Instead, we adopted a different approach by measuring the energy intervals between the peaks on the low binding energy side and the peaks on the high binding energy side in Figure 1, which allows for the accumulation of the anharmonic offset. For example, the vibrational quantum number differences Δv between peaks *a* and *i*, and between peaks *b* and *j*, are both 8. If the high-order anharmonic terms are temporarily ignored, the accumulated anharmonic offset for the energy interval between the two groups of peaks is roughly estimated to be $16\omega_e\chi_e$. The derivation is presented in the Supporting Information. To accurately measure the binding energies of peaks *a*, *b*, and *c* as well as peaks *i* and *j*, we acquired the spectra near their respective photodetachment thresholds. As depicted in Figure 1, these spectra exhibit sharp peaks. To determine the vibrational quantum numbers, we employed the successive difference method. By cross-subtracting the binding energies of the two groups of peaks in Figure 1, we obtained a series of vibrational energy intervals, which are presented in Table 1 and Figure 2. The vibrational quantum number (v) corresponding to a specific peak can be unambiguously determined by comparing the measured vibrational energy interval in the present experiment with that calculated one using eq 2. For example, the measured energy interval between peaks *a* and *i* is 3455 cm^{-1}, and vibrational quantum number difference Δv between these two peaks is 8 according to Figure 1. By drawing a horizontal line with an energy 3455 cm^{-1} and intersecting the curve for Δv = 8, we obtain the vibrational number v_1 = 17 of peak *a*. By referring to Table S2 of the Supporting Information, we find that the closest match to the energy interval with Δv = 8 is 3460.05 cm^{-1}. Consequently, the vibrational numbers of peaks *a* and *i* were assigned to 17 and

https://doi.org/10.1021/acs.jpclett.4c01821
J. Phys. Chem. Lett. 2024, 15, 7735−7739

Table 1. Determination of Vibrational Quantum Numbers Corresponding to Experimentally Precisely Measured Peaks a, b, c, i, and j Utilizing the Method of Successive Difference

Peaks	Measured binding energy interval (cm^{-1})	Vibrational energy interval calculated using Eq. 2 (cm^{-1})	Δv	$v_1 - v_2$
$a - i$	3455	3460.05	8	17 − 25
$b - i$	3002	3004.45	7	18 − 25
$c - i$	2558	2555.27	6	19 − 25
$a - j$	3851	3861.62	9	17 − 26
$b - j$	3398	3406.03	8	18 − 26
$c - j$	2954	2956.85	7	19 − 26

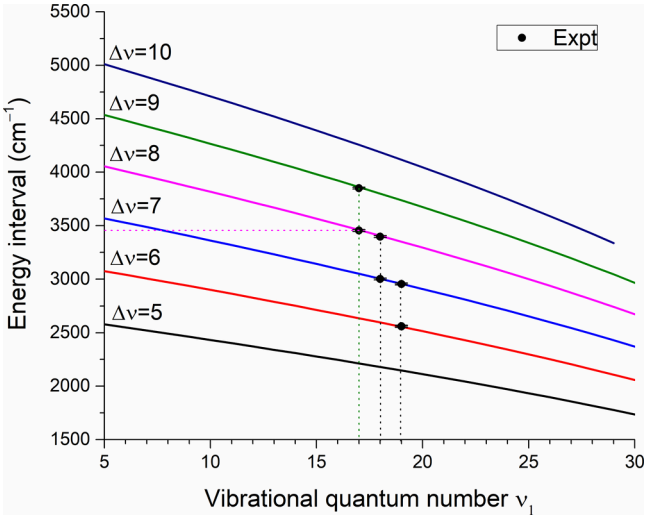

Figure 2. Schematic for determining the vibrational quantum numbers of Cl_2 using the successive difference method. The curves are generated using the data in Table S2 of the Supporting Information based on the Eq. 2. The dotted lines are for guiding the eyes.

25, respectively. By using the successive difference method, we can determine the vibrational numbers of all observed peaks, as indicated by the vertical bars in Figure 1.

Given the precise vibrational energy level of the neutral Cl_2, the EA value of Cl_2 can be obtained by subtracting the neutral vibrational energy from the measured binding energy of each peak. Figure 3 shows the EA values obtained at different vibrational transitions. The average EA value of Cl_2 is determined to be 19432(9) cm^{-1}, or 2.4093(11) eV. The uncertainty includes the statistical uncertainty and the systematic uncertainty arising from the OPO laser line width (6 cm^{-1}). Notably, another data point for v = 19 was independently measured on a separate day to verify its reliability, demonstrating excellent agreement between measurements.

The measured EA value is compared with previous results in Table 2. Our result aligns reasonably well with most of the previously reported findings, except for 1.02(5) eV by Hubers et al. in 1976[21] and 3.20(20) eV by Lacmann and Herschbach in 1970,[18] but with an improved accuracy by 2 orders of magnitude. The EA values predicted by theoretical calculations are also summarized in Table S3 of the Supporting Information. It can be found that the EA value (2.408 eV) calculated via the CCSD(T) method by Leininger et al. is in excellent agreement with our measured value 2.4093 eV.[12] Table 3 summarizes the spectroscopic constants of the ground state ($X'\ ^2\Sigma_u^+$) of anionic Cl_2^- calculated using quantum chemical methods, along with those of the neutral ground state ($X\ ^1\Sigma_g^+$) obtained from the NIST database.[36,37] The equilibrium bond length r_e and the harmonic vibrational constant ω_e of Cl_2^- were optimized at the CCSD(T)-F12/VTZ level of theory using the Molpro software package.[38] The anharmonic constant $\omega_e\chi_e$ was derived from the following equations:

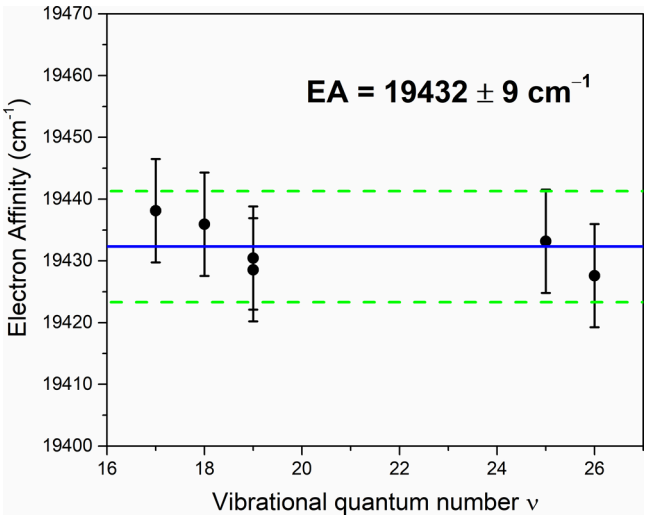

Figure 3. EA of Cl_2 determined using different vibrational energy levels. The blue line indicates the average value of the EA. The dashed lines indicate the ±9 cm^{-1} uncertainty.

Table 2. Summary of the Experimental EA Values of Cl_2

Value	Methods[a]	References
3.20(20) eV	NBIE	Lacmann and Herschbach, 1970[18]
2.38(10) eV	Endo	Chupka et al., 1971[19]
2.52(17) eV	EIAE	DeCorpo and Franklin, 1971[13]
2.45(15) eV	NBIE	Baede, 1972[14]
2.46(14) eV	IMRB	Dunkin et al., 1972[15]
2.32(10) eV	Endo	Hughes et al., 1973[20]
1.02(5) eV	NBIE	Hubers et al., 1976[21]
2.40(20) eV	NBIE	Dispert and Lacmann, 1977[39]
2.33 eV	ECD	Ayala et al., 1981[40]
2.50(20) eV	NBIE	Bowen et al., 1983[17]
2.4093(11) eV or 19432(9) cm^{-1}	SEVI	This work

[a]Abbreviations: NBIE, neutral beam ionization potentials; Endo, Translational threshold for endothermic ion/molecule process; EIAE, Electron impact appearance energy; IMRB, Ion/molecule reaction bracketing; ECD: Electron capture detector; SEVI: slow-electron velocity-map imaging.

Table 3. Spectroscopic Constants of Anionic Cl_2^- and Neutral Cl_2[a]

	Electronic state	Experimental gap (cm^{-1})	r_e (Å)	ω_e (cm^{-1})	$\omega_e\chi_e$ (cm^{-1})
Cl_2^-	$X'\ ^2\Sigma_u^+$	0	2.576[b]	260.76[b]	1.63[c]
Cl_2	$X\ ^1\Sigma_g^+$	19432(9)	1.987	559.7	2.67

[a]Spectroscopic constants of neutral Cl_2 are obtained from the NIST database.[36,37] [b]The equilibrium bond length and the harmonic vibrational constant are from quantum chemical calculations. [c]The anharmonic constant $\omega_e\chi_e$ is calculated via the eqs 3 and 4.

https://doi.org/10.1021/acs.jpclett.4c01821
J. Phys. Chem. Lett. 2024, 15, 7735−7739

$$\omega_e\chi_e = \frac{\omega_e v_0}{4D_0} \quad (3)$$

$$v_0 = \frac{2D_0\omega_e}{2D_0 + \omega_e} \quad (4)$$

Here D_0 represents the dissociation energy of Cl_2^-, obtained using the relation: $D_0(Cl_2^-) = EA(Cl_2) - EA(Cl) + D_0(Cl_2)$. With $EA(Cl_2)$ determined in our experiment and the literature values of 3.612725(28) eV for EA(Cl)[31] and 2.4793 eV for $D_0(Cl_2)$,[10] we obtained the value of $D_0(Cl_2^-)$ to be 1.2759 eV. Furthermore, the fundamental vibrational frequency of Cl_2^- was calculated as 257.50 cm^{-1} via eq 4.

In summary, using the high-resolution cryo-SEVI spectroscopy and the successive difference method, we have determined the precise EA value of chlorine molecule Cl_2 to be 19432(9) cm^{-1} or 2.4093(11) eV. Given the absence of accurate experimental EA data for F_2 and Br_2, we plan to employ the same method to measure their electron affinities.

■ ASSOCIATED CONTENT

Data Availability Statement

The data that supports the findings of this study are available within the article and its Supporting Information.

Supporting Information

The Supporting Information is available free of charge at https://pubs.acs.org/doi/10.1021/acs.jpclett.4c01821.

Derivation of accumulated offset $16\omega_e\chi_e$; a summary of the Dunham coefficients of the ground state X $^1\Sigma_g^+$ of Cl_2; detailed data on the vibrational energy level and their intervals calculated by eq 2; summary of the calculated EA values of Cl_2; and the Franck−Condon simulation (PDF)

■ AUTHOR INFORMATION

Corresponding Author

Chuangang Ning − *Department of Physics, State Key Laboratory of Low Dimensional Quantum Physics, Frontier Science Center for Quantum Information, Tsinghua University, Beijing 100084, China;* orcid.org/0000-0002-3158-1253; Email: ningcg@tsinghua.edu.cn

Authors

Shuaiting Yan − *Department of Physics, State Key Laboratory of Low Dimensional Quantum Physics, Frontier Science Center for Quantum Information, Tsinghua University, Beijing 100084, China*

Rui Zhang − *Department of Physics, State Key Laboratory of Low Dimensional Quantum Physics, Frontier Science Center for Quantum Information, Tsinghua University, Beijing 100084, China;* orcid.org/0000-0001-9080-4528

Complete contact information is available at: https://pubs.acs.org/10.1021/acs.jpclett.4c01821

Notes

The authors declare no competing financial interest.

■ ACKNOWLEDGMENTS

This work was s supported by the National Natural Science Foundation of China (NSFC) (Grant Nos. 12374244 and 12341401) and the Postdoctoral Fellowship Program of CPSF (Grant No. GZC20231367).

■ REFERENCES

(1) Ning, C.; Lu, Y. Electron Affinities of Atoms and Structures of Atomic Negative Ions. *J. Phys. Chem. Ref. Data* **2022**, *51*, 021502.

(2) Yan, S.; Lu, Y.; Zhang, R.; Ning, C. Electron Affinities in the Periodic Table and an Example for As. *Chin. J. Chem. Phys.* **2024**, *37*, 1−12.

(3) Rienstra-Kiracofe, J. C.; Tschumper, G. S.; Schaefer, H. F.; Nandi, S.; Ellison, G. B. Atomic and Molecular Electron Affinities: Photoelectron Experiments and Theoretical Computations. *Chem. Rev.* **2002**, *102*, 231−282.

(4) Yan, S.; Zhang, R.; Lu, Y.; Ning, C. Spectroscopic observation of Feshbach resonances in the tellurium dimer anion. *J. Chem. Phys.* **2024**, *160*, 064303.

(5) Ervin, K. M.; Anusiewicz, I.; Skurski, P.; Simons, J.; Lineberger, W. C. The Only Stable State of O_2^- Is the X $^2\Pi_g$ Ground State and It (Still!) Has an Adiabatic Electron Detachment Energy of 0.45 eV. *J. Phys. Chem. A* **2003**, *107*, 8521−8529.

(6) Zanni, M. T.; Taylor, T. R.; Greenblatt, B. J.; Soep, B.; Neumark, D. M. Characterization of the I_2^- anion ground state using conventional and femtosecond photoelectron spectroscopy. *J. Chem. Phys.* **1997**, *107*, 7613−7619.

(7) Clark, A. P.; Brouard, M.; Quadrini, F.; Vallance, C. Atomic polarization in the photodissociation of diatomic molecules. *Phys. Chem. Chem. Phys.* **2006**, *8*, 5591−5610.

(8) Machado, D. F. S.; Silva, V. H. C.; Esteves, C. S.; Gargano, R.; Macedo, L. G. M.; Mundim, K. C.; de Oliveira, H. C. B. Fully relativistic rovibrational energies and spectroscopic constants of the lowest X:$(1)0_g^+$, A′:$(1)2_u$, A:$(1)1_u$, B′:$(1)0_u^-$ and B:$(1)0_u^+$ states of molecular chlorine. *J. Mol. Model.* **2012**, *18*, 4343−4348.

(9) Shi, D.-H.; Zhang, X.-N.; Liu, H.; Zhu, Z.-L.; Sun, J.-F. Theoretical investigations of spectroscopic parameters and molecular constants for electronic ground state of Cl_2 and its isotopes. *Chin. Phys. B* **2010**, *19*, 103401.

(10) Christophorou, L. G.; Olthoff, J. K. Electron Interactions With Cl_2. *J. Phys. Chem. Ref. Data* **1999**, *28*, 131−169.

(11) Gutsev, G. L. The structure and stability of Cl_n^- clusters, n = 2−7. *Chem. Phys.* **1991**, *156*, 427−437.

(12) Leininger, T.; Gadéa, F. X. *Ab initio* calculations for electron attachment to Cl_2. *J. Phys. B: At., Mol. Opt. Phys.* **2000**, *33*, 735.

(13) DeCorpo, J. J.; Franklin, J. L. Electron Affinities of the Halogen Molecules by Dissociative Electron Attachment. *J. Chem. Phys.* **1971**, *54*, 1885−1888.

(14) Baede, A. P. M. The adiabatic electron affinities of Cl_2, Br_2, I_2, IBr, NO_2 and O_2. *Physica* **1972**, *59*, 541−544.

(15) Dunkin, D. B.; Fehsenfeld, F. C.; Ferguson, E. E. Thermal energy rate constants for the reactions $NO_2^- + Cl_2 \rightarrow Cl_2^- + NO_2$, $Cl_2^- + NO_2 \rightarrow Cl^- + NO_2Cl$, $SH^- + NO_2 \rightarrow NO_2^- + SH$, $SH^- + Cl_2 \rightarrow Cl_2^- + SH$, and $S^- + NO_2 \rightarrow NO_2^- + S$. *Chem. Phys. Lett.* **1972**, *15*, 257−259.

(16) Gutsev, G. L. Structures of CCl_n^- and Cl_n^- anions (n = 1−4) according to results of local density functional calculations. *J. Phys. Chem.* **1991**, *95*, 5773−5783.

(17) Bowen, K. H.; Liesegang, G. W.; Sanders, B. S.; Herschbach, D. R. Electron attachment to molecular clusters by collisional charge transfer. *J. Phys. Chem.* **1983**, *87*, 557−565.

(18) Lacmann, K.; Herschbach, D. R. Collisional excitation and ionization of K atoms by diatomic molecules: Role of ion-pair states. *Chem. Phys. Lett.* **1970**, *6*, 106−110.

(19) Chupka, W. A.; Berkowitz, J.; Gutman, D. Electron Affinities of Halogen Diatomic Molecules as Determined by Endoergic Charge Transfer. *J. Chem. Phys.* **1971**, *55*, 2724−2733.

(20) Hughes, B. M.; Lifshitz, C.; Tiernan, T. O. Electron affinities from endothermic negative-ion charge-transfer reactions. III. NO, NO_2, SO_2, CS_2, Cl_2, Br_2, I_2, and C_2H. *J. Chem. Phys.* **1973**, *59*, 3162−3181.

(21) Hubers, M. M.; Kleyn, A. W.; Los, J. Ion pair formation in alkali-halogen collisions at high velocities. *Chem. Phys.* **1976**, *17*, 303−325.

(22) Osterwalder, A.; Nee, M. J.; Zhou, J.; Neumark, D. M. High resolution photodetachment spectroscopy of negative ions via slow photoelectron imaging. *J. Chem. Phys.* **2004**, *121*, 6317−6322.
(23) Wang, X.-B.; Wang, L.-S. Development of a low-temperature photoelectron spectroscopy instrument using an electrospray ion source and a cryogenically controlled ion trap. *Rev. Sci. Instrum.* **2008**, *79*, 073108.
(24) Hock, C.; Kim, J. B.; Weichman, M. L.; Yacovitch, T. I.; Neumark, D. M. Slow photoelectron velocity-map imaging spectroscopy of cold negative ions. *J. Chem. Phys.* **2012**, *137*, 244201.
(25) Weichman, M. L.; Neumark, D. M. Slow Photoelectron Velocity-Map Imaging of Cryogenically Cooled Anions. *Annu. Rev. Phys. Chem.* **2018**, *69*, 101−124.
(26) Chen, X.; Ning, C. Accurate electron affinity of Co and fine-structure splittings of Co^- via slow-electron velocity-map imaging. *Phys. Rev. A* **2016**, *93*, 052508.
(27) Tang, R.; Fu, X.; Ning, C. Accurate electron affinity of Ti and fine structures of its anions. *J. Chem. Phys.* **2018**, *149*, 134304.
(28) Zhang, R.; Yan, S.; Song, H.; Guo, H.; Ning, C. Probing the activated complex of the F + NH_3 reaction via a dipole-bound state. *Nat. Commun.* **2024**, *15*, 3858.
(29) Wiley, W. C.; McLaren, I. H. Time-of-Flight Mass Spectrometer with Improved Resolution. *Rev. Sci. Instrum.* **1955**, *26*, 1150−1157.
(30) Eppink, A. T. J. B.; Parker, D. H. Velocity map imaging of ions and electrons using electrostatic lenses: Application in photoelectron and photofragment ion imaging of molecular oxygen. *Rev. Sci. Instrum.* **1997**, *68*, 3477−3484.
(31) Berzinsh, U.; Gustafsson, M.; Hanstorp, D.; Klinkmüller, A.; Ljungblad, U.; Mårtensson-Pendrill, A. M. Isotope shift in the electron affinity of chlorine. *Phys. Rev. A* **1995**, *51*, 231−238.
(32) Dick, B. Inverting ion images without Abel inversion: maximum entropy reconstruction of velocity maps. *Phys. Chem. Chem. Phys.* **2014**, *16*, 570−580.
(33) Tang, R.; Fu, X.; Lu, Y.; Ning, C. Accurate electron affinity of Ga and fine structures of its anions. *J. Chem. Phys.* **2020**, *152*, 114303.
(34) Dunham, J. L. The Energy Levels of a Rotating Vibrator. *Phys. Rev.* **1932**, *41*, 721−731.
(35) Douglas, A. E.; Hoy, A. R. The Resonance Fluorescence Spectrum of Cl_2 in the Vacuum Ultraviolet. *Can. J. Phys.* **1975**, *53*, 1965−1975.
(36) Huber, K. P.; Herzberg, G. *Molecular spectra and molecular structure: IV. Constants of diatomic molecules*; Van Nostrand: New York, 1979.
(37) Clyne, M. A. A.; Coxon, J. A. The visible band absorption spectrum of chlorine. *J. Mol. Spectrosc.* **1970**, *33*, 381−406.
(38) Werner, H.-J.; Knowles, P. J.; Knizia, G.; Manby, F. R.; Schütz, M. Molpro: a general-purpose quantum chemistry program package. *WIREs Comput. Mol. Sci.* **2012**, *2*, 242−253.
(39) Dispert, H.; Lacmann, K. Chemiionization in alkali-halogen reactions: Evidence for ion formation by alkali dimers. *Chem. Phys. Lett.* **1977**, *47*, 533−536.
(40) Ayala, J. A.; Wentworth, W. E.; Chen, E. C. M. Electron attachment to halogens. *J. Phys. Chem.* **1981**, *85*, 768−777.

https://doi.org/10.1021/acs.jpclett.4c01821
J. Phys. Chem. Lett. 2024, 15, 7735−7739